

Harnessing Monocytes for a Liposomal Rosiglitazone-Mediated Anti-Inflammatory Effect

Osnat Shvindelman¹, Mirjam M. Nordling-David¹, Ety Grad¹ and Gershon Golomb^{*1,2}

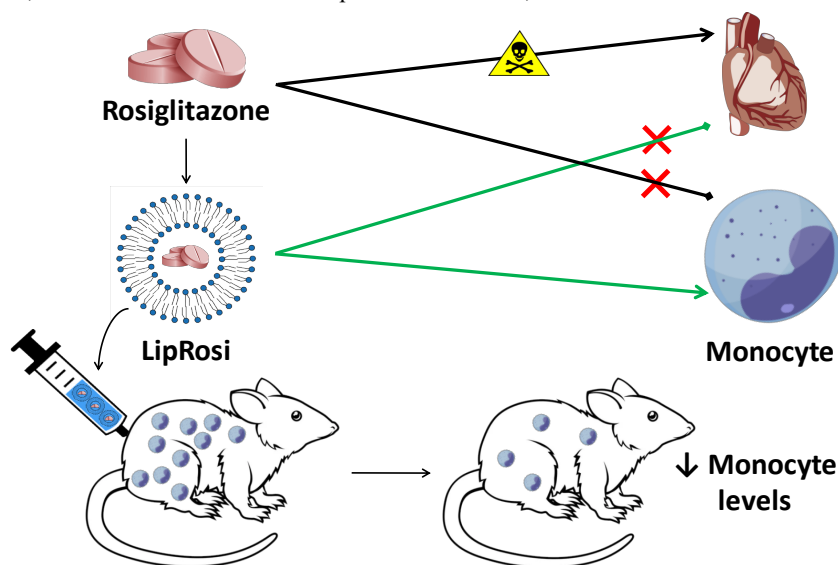
¹*Institute for Drug Research, School of Pharmacy, Faculty of Medicine, The Hebrew University of Jerusalem, Jerusalem 9112001, Israel.*

²*The Center for Nanoscience and Nanotechnology, The Hebrew University of Jerusalem, Jerusalem 9190401, Israel.*

Submitted: July 28, 2022

Accepted: November 27, 2022

Published: November 28, 2022



Abstract

Rosiglitazone, an anti-diabetic drug used for treating type II diabetes mellitus with known anti-inflammatory properties, was withdrawn from the European market. The United States Food and Drug Administration has restricted its use due to its severe cardiovascular adverse effects. We hypothesized that rosiglitazone could be repurposed to provide safe anti-inflammatory therapy. By encapsulating the drug in liposomes internalized preferentially by circulating monocytes, monocytes' inhibition can be achieved while avoiding the inherent systemic side effects. Rosiglitazone was loaded into empty liposomes by an active loading method. The formulation (LipRosi) was developed with desirable physicochemical properties promoting preferential monocyte internalization via membrane surface negative charge. Appropriate physicochemical properties include nano-size, low polydispersity index (PDI), high drug loading capacity, high encapsulation yield, and shelf-life stability. Further, these liposomes exhibited time- and concentration-dependent uptake in a murine monocyte/macrophage cell line (RAW264.7). In addition, LipRosi was found to be significantly more effective in depleting monocytes than drug-free liposomes and the free drug in solution. A cytotoxic effect on smooth muscle cells was only observed at the highest concentration examined and after an extended exposure time. In vivo studies in rats demonstrated a time-dependent uptake by intact circulating white blood cells (WBC), primarily monocytes. Administration of 20 mg/kg LipRosi, injected on two consecutive days, achieved a therapeutic window of monocyte depletion after 24 hr. Of note, only a dismal disposition of the formulation was detected in the heart. Since monocytes play a central role in the progression of inflammatory related-disorders, LipRosi could be found therapeutic for multiple disorders.

Keywords: rosiglitazone, liposomes, drug delivery system, anti-inflammation

*Correspondence: gershon.golomb@mail.huji.ac.il; Tel.: +972-2-675-8658

Rationale and purpose

Rosiglitazone, an effective anti-diabetic drug with anti-inflammatory properties, has been withdrawn from the European market, and the FDA has restricted its use due to its severe cardiovascular adverse effects. However, redirecting the drug away from the heart towards specific sites such as the mononuclear phagocyte system (MPS) may be achieved by its encapsulation in nanoparticles (NPs), thus maximizing its anti-inflammatory properties while avoiding systemic side effects. We herein present a novel liposomal formulation containing rosiglitazone that preferentially inhibits circulating monocytes, demonstrating a potential for safe anti-inflammatory therapy.

Introduction

Macrophages and their monocyte precursors are professional phagocytic cells of the MPS (1-3). Monocytes and macrophages play central roles in initiating, progressing, and resolving inflammation, principally through phagocytosis, releasing inflammatory cytokines, and activating the acquired immune system (4, 5). Due to their significant involvement in the pathogenesis of inflammation-driven pathological conditions, monocytes are potential therapeutic targets (4, 6-9). In addition, depletion of monocytes following preferential phagocytosis of NPs containing anti-inflammatory agents is beneficial in inflammatory-associated disorders, including cardiovascular disorders (1, 10-12), rheumatoid arthritis (13), and endometriosis (14).

Rosiglitazone, a member of the thiazolidinedione class of drugs, is a peroxisome proliferator-activated receptor γ (PPAR γ) agonist. Unfortunately, rosiglitazone's clinical use for treating type II diabetes mellitus has been suspended by the European Medicines Agency since significant safety concerns have been raised due to its cardiovascular toxicity (15-18). PPAR γ , a key regulator of glucose homeostasis and lipid metabolism, is also expressed in multiple immune cells, including monocytes/macrophages (19). In addition, PPAR γ agonists act as negative regulators of macrophages and inhibit the production of pro-inflammatory cytokines (20-22). Rosiglitazone was shown to have an anti-inflammatory effect via modulation of nuclear factor kappa-B (NF- κ B) and NF- κ B inhibitor (I κ B) (23). Therefore, we hypothesized

that directing the drug preferentially to monocytes, using a suitable delivery system, has the potential to maximize its anti-inflammatory potency and concomitantly avoid undesired effects. This can be achieved by encapsulating rosiglitazone in liposomes targeting circulating monocytes. The subsequent inhibition of monocytes/macrophages, bypassing drug accumulation in the heart and its inherent side effects, could result in the repurposing of rosiglitazone as an anti-inflammatory agent.

To our knowledge, this is the first report on a rosiglitazone formulation for monocyte depletion. The formulation was characterized in terms of its physicochemical properties, stability, uptake, and bioactivity were evaluated both *in vitro* and *in vivo*.

Experimental design

We developed a monocyte-targeted delivery system of negatively-charged liposomes encapsulating rosiglitazone in the aqueous core. The drug was loaded into liposomes by an active loading method. The formulation was characterized in terms of its physicochemical properties, stability, cellular uptake, bioactivity, and cytotoxicity *in vitro*. In addition, its biodistribution and bioactivity have been further examined *in vivo*.

Materials and methods

Liposome preparation

Rosiglitazone maleate-loaded liposomes were formulated using an active loading method in a two-step process (24). In the 1st step, calcium acetate-loaded liposomes were assembled, and in the 2nd step, liposomes exhibiting transmembrane calcium acetate gradient were incubated with a rosiglitazone maleate solution for remote drug loading. Negatively charged liposomes were prepared by the modified film thin hydration method (25, 26). Liposomes were composed of 1,2-distearoyl-*sn*-glycero-3-phosphocholine (DSPC; Lipoid, Ludwigshafen, Germany), 1,2-distearoyl-*sn*-glycero-3-phospho-(1'-*rac*-glycerol) (DSPG; Lipoid) and cholesterol (Sigma-Aldrich, Israel), at a molar ratio of 3:1:2, respectively. Lipids were dissolved in *tert*-butyl alcohol (Sigma-Aldrich), lyophilized overnight, and the obtained film was hydrated with 120 mM calcium acetate (Sigma-Aldrich) solution and then rotated in a bath (70°C at 90

rpm for 40 min). The size of the obtained multilamellar vesicles was reduced using a thermo-barrel extruder (LipexBiomembranes, Vancouver, Canada), at 70°C, through double polycarbonate membranes of 0.8 and 0.4 μm ($\times 2$ times each), followed by 0.2 μm ($\times 6$ times), yielding small unilamellar liposomes. The liposomal suspension was dialyzed overnight against water to create a transmembrane calcium acetate gradient (10 mm diameter, 25K membrane; Spectrum Laboratories, USA).

Remote drug loading

Rosiglitazone maleate (Abcam, UK) solution (dissolved in citrate buffer, pH 3) was mixed with a preformed liposome suspension, reaching a final 10 mg/ml drug concentration in the suspension (4 hr at RT). Next, the free, unencapsulated drug was removed through a citrate buffer (pH 3) dialysis overnight. Finally, the liposomes were dialyzed against phosphate-buffered saline (PBS) (Biological Industries, Israel), as described above.

A filter spin column concentrator (Vivaspin, 300,000 MW; Sartorius Stedim Lab Ltd, UK) was used to increase liposomal drug concentration. Liposomes were centrifuged at 3000 g up until leaving a calculated lipid concentration of 50 mg/mL. The obtained liposomal suspension (LipRosi) was filter-sterilized and stored at 4°C until used.

Drug-free liposomes (Empty Lip) were prepared similarly by omitting the drug. Fluorescent double-labeled empty liposomes (rhodamine and Cy5, membrane and aqueous core, respectively; LipRhod-Cy5) were prepared similarly by (i) adding the lipophilic fluorescent marker, 1,2-dioleoyl-*sn*-glycero-3-phosphoethanolamine-N-(lissamine rhodamine B sulfonyl) (PE-rhodamine; Avanti) to the dissolved lipids in *tert*-butyl alcohol at a molar ratio of 3:1:2:0.08 (DSPC:DSPE:Cholesterol:PE-rhodamine, respectively); and (ii) hydrating the film with 0.5 mM Cy5 (Lumiprobe, USA) dissolved in 120 mM calcium acetate solution.

Drug loading and encapsulation yield

Encapsulated rosiglitazone concentration was determined using HPLC (2695 eAlliance separation module, Waters Corporation, MA, USA). A filter spin column concentrator (Vivaspin, 50,000 MW; Sartorius Stedim Lab Ltd, UK) was used to determine the drug concentration inside and outside the vesicles. Liposomes were

centrifuged for 40 min at 3000 relative centrifugal force to separate the external buffer from the vesicles. In another tube, liposomes were disrupted by adding acetonitrile (JT Baker, Avantor, USA), yielding a clear solution. Equal liposome suspension or external buffer volumes were injected into a Hypersil BDS C18 column (250 \times 4.6 mm, 5 μm , Thermo Scientific, USA). The column was eluted with a mixture of 20% acetonitrile and 80% acetate buffer pH 4, at a flow rate of 1 ml/min. Rosiglitazone was detected at $\lambda=210$ nm using a 2998 PDA detector (Waters Corporation, UK).

Size, polydispersity index, zeta potential, and morphology

Liposome size, polydispersity index (PDI), and zeta potential were determined by dynamic light scattering at room temperature following 1:100 dilution with PBS (Zetasizer Nano-ZSP, Malvern Instruments, Malvern, UK).

The liposome morphology was examined through cryogenic transmission electron microscopy (Cryo-TEM). On a glow discharged TEM grid (300-mesh Cu grid) coated with a perforated carbon film (Lacey substrate, Ted Pella, Inc., USA), a drop (3 μL) of the samples was applied. After blotting excess liquid, the samples were vitrified by rapidly dipping them into liquid ethane pre-cooled with liquid nitrogen using Vitrobot Mark IV (FEI, USA). Samples were examined using Tecnai G2 12 TWIN TEM equipped with Gatan 626 cold stage at -177°C . Images were recorded (4 K \times 4 K FEI Eagle CCD camera) at 120 kV in a low-dose mode.

Stability

Shelf-life stability of LipRosi, stored at 4°C, was determined by examining changes of vesicle size, PDI, and zeta potential. LipRosi liposomes were diluted in fetal bovine serum (FBS; Biological Industries, Israel) at a ratio of 1:10 and incubated at 37°C for 24 and 48 hr. The dilution factor was chosen based on the maximal estimated incubation concentration of liposomes per well in vitro. The affinity of serum proteins to LipRosi was evaluated as a function of the liposome size distribution pre- and post-incubation period and was measured using a Zetasizer. The results were compared to negatively-charged drug-free liposomes (Empty Lip) that underwent the same procedure.

Cell culture studies

Bioactivity

The bioactivity was evaluated by means of the MTT assay using a murine monocyte/macrophage cell line (RAW264.7, ATCC, Rockville, MD, USA). RAW264.7 cells were grown in Dulbecco's modified eagle medium (DMEM; Biological Industries, Israel), enriched with 10% FBS, 2 mM L-glutamine, 100 units/mL penicillin, and 100 µg/mL streptomycin in 5% CO₂ atmosphere at 37°C. Cells were seeded in 96-well plates (10,000 cells/well) containing DMEM supplemented with 10% FBS and treated the following day with LipRosi, Empty Lip, and Free Rosi solution diluted in DMEM for 24 and 48 hr. Dimethyl sulfoxide (DMSO; Sigma-Aldrich) served as a positive control (10% v/v).

After incubation, cells were washed, and 10% thiazolyl blue tetrazolium bromide (MTT, Sigma-Aldrich) was added to each well and incubated for 60 min. After the removal of unreacted dye, 100 µl/well DMSO was added, and the purple formazan product was dissolved using an orbital shaker for 15 min at 37°C. The plates were then quantified using a plate reader (Cytation 3, BioTrek) at $\lambda=540$ nm, and the value of viable cells was normalized to non-treated cells.

Cellular uptake

RAW264.7 cells were seeded on coverslips in 12-well plates (100,000 cells/well), containing DMEM supplemented with 10% FBS. Cells were treated the following day with LipRhod-Cy5 (0.5 and 1.25 mg/mL lipid concentration). At the end of the incubation periods (4 and 24 hr), cells were washed with PBS (3×), fixed with 4% formaldehyde solution (Sigma-Aldrich, Israel), washed with PBS (3×), and stained with 10 µg/mL Hoechst reagent (nuclear staining, Sigma-Aldrich, Israel) followed by a wash with PBS (2×). Each coverslip was mounted on a microscope slide with 8 µL Fluoromount-G solution (Invitrogen, Thermo Fisher Scientific, USA), and the slides were examined using an Olympus FV 10i confocal laser scanning microscope 1 × 60 (Olympus America, Inc., MA, USA). This was followed by image analysis using the Olympus FV10-ASW 3.1 viewer software.

Cytotoxicity

The cytotoxicity was evaluated using the MTT assay on primary rat smooth muscle cells (SMC) isolated from the aorta of Sabra male rats (Harlan Laboratories, Jerusalem, Israel), as previously described (27). SMC were seeded in 96-well plates (5,000 cells/well) containing DMEM supplemented with 15% FBS and 5 µl/mL fibronectin (Biological Industries, Israel). Cells were treated the following day with LipRosi, Empty Lip, and Free Rosi solution diluted in the medium. DMSO served as the positive control (10% v/v). After incubation (24 and 48 hr), the results were analyzed as described in the "bioactivity" section.

In vivo studies

In all experiments, male sabra rats (Harlan Laboratories) were randomly divided into subgroups and treated by an IV injection into the tail vein. Animals were fed with standard laboratory chow and tap water *ad libitum*. Animal care and procedures conformed to the standards for care and use of laboratory animals of the Hebrew University of Jerusalem and the National Instituted of Health (NIH, USA).

Biodistribution

Rats (250–300 g) were administered intravenously with 1.5 mL LipRhod-Cy5 (n=6). Rats injected with saline (n=2) served as control. Animals were sacrificed 6 and 24 hr post-treatment and were perfused via the left ventricle with saline. Selected internal organs were harvested (liver, kidneys, lungs, spleen, and heart) and washed with saline. Organs were scanned utilizing a Typhoon scanner at ex550nm/em570nm and ex650/em670, followed by ImageJ analysis. The relative fluorescence intensity was calculated by subtracting a control organ's fluorescence intensity from the tested organ's fluorescence intensity.

Uptake of the liposomes by WBC was evaluated in the same rats. Heparinized blood was drawn 6 and 24 hr post-injection by cardiac puncture under isoflurane anesthesia (Minrad International USA). Red blood cells were lysed (Erythrolyse, 1:20 dilution, AbD, Serotec, UK) for 10 min at room temperature, and the pellet was washed twice with flow cytometry (FACS) medium (PBS, 1% BSA, 0.02% sodium azide). The samples were analyzed using LSRII (BD Biosciences), and the FCS Express 4 software was used for quantitative analysis. The total

white blood cell (WBC) count was gated according to forward and side scattering. Monocyte, granulocyte, and lymphocyte populations were gated according to their typical forward and side scattering. The fraction of Cy5-containing WBC was calculated as the number of cells stained positive for Cy5 divided by the number of gated cells.

Bioactivity

The bioactivity of LipRosi in terms of monocyte depletion was studied in 3 different experiments. In the first experiment, intact sabra male rats (300–350 g) were treated with a single injection of LipRosi (10 mg/kg; n=9) or saline (n=6). A similar protocol was used in the second experiment, but the rats (270–300 g) were treated with a single, double dose of LipRosi (20 mg/kg). Finally, in the third experiment, rats (180–245 g) were treated with two injections of 20 mg/kg LipRosi (n=8), Free Rosi (n=6), drug-free liposomes (Empty Lip; n=3), or saline (n=6) on two consecutive days.

Monocytes analysis

Blood specimens were drawn from the tail under isoflurane anesthesia at baseline and specified time points in heparinized vials. The blood specimens (50 µL) were incubated with red blood cell lysing solution (1:20 dilution) for 10 min at room temperature. Next, the cells were washed and suspended in 1 mL FACS medium

(PBS, 1% BSA, 0.02% sodium azide, 0.1% saponin). The cells were centrifuged at 8000 g for 1 min and then incubated for 30 min with Alexa Fluor 647-conjugated anti-ED1 and the respective isotype-matched negative control, IgG1-Alexa Fluor 647 (AbD Serotec, UK). At the end of incubation, cells were washed and resuspended in FACS medium (omitting the saponin). Total monocytes were classified as positive to anti-ED1. The samples were analyzed using LSRII, and the FCS Express 4 software was used for quantitative analysis.

Statistical analysis

All data are expressed as mean ± standard deviation unless otherwise noted. Comparisons among treatment groups were made by two-way analysis of variance (ANOVA) followed by the Tukey test and the Student's t-test for independent means when necessary. Differences were termed statistically significant at $p < 0.05$.

Results

Liposomes characterization

Negatively-charged liposomes containing rosiglitazone (LipRosi) obtained by the active loading method demonstrated desirable physicochemical properties, including high encapsulation yield (~50%), a negative zeta potential (-21.3 ± 1.3 mV), and a mean diameter of ~170 nm with PDI <0.1 (Table 1).

Table 1: The physicochemical properties of liposomal rosiglitazone, empty liposomes, and fluorescently labeled liposomes. Data is presented as the mean ± SD.

Formulation	LipRosi	Empty Lip	LipRhod-Cy5
Composition	DSPC:DSPG:Cholesterol	DSPC:DSPG:Cholesterol	DSPC:DSPG:Cholesterol:PE-Rhodamine
Molar ratio	3:1:2	3:1:2	3:1:2:0.008
Size (nm)	172.8 ± 3.0	133.3 ± 0.9	150.9 ± 2.6
Polydispersity Index (PDI)	0.075 ± 0.009	0.068 ± 0.003	0.075 ± 0.030
ζ potential (mV)	-21.3 ± 1.3	-22.9 ± 1.0	-22.5 ± 0.7
Drug encapsulated (mg/ml)	5.1	-	-
Encapsulation yield (%)	51.5	-	-

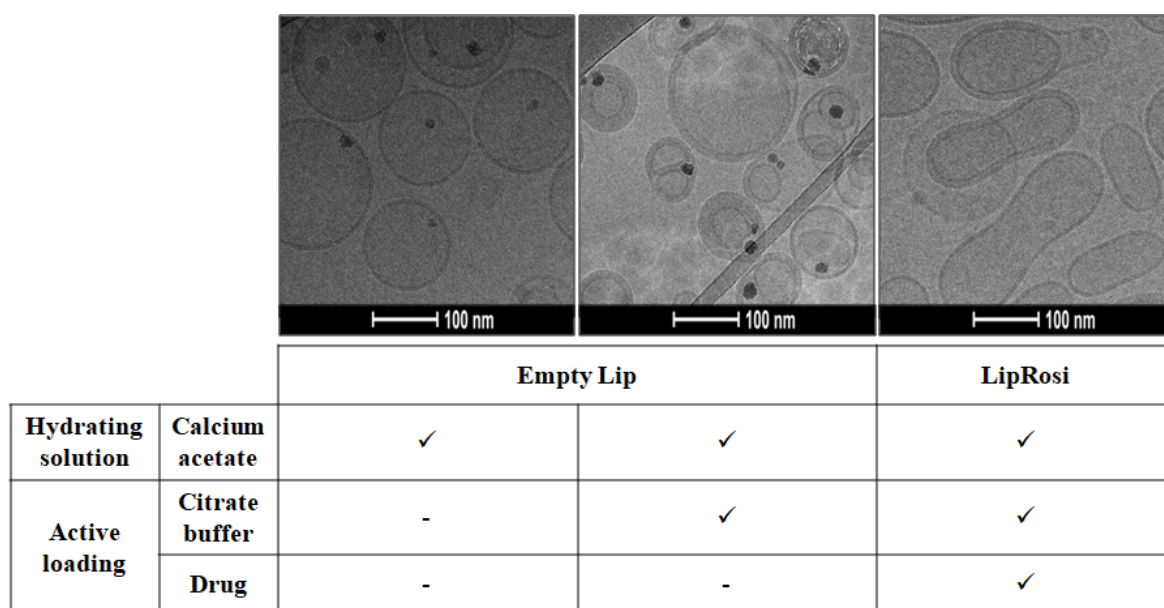


Figure 1. Representative cryogenic transmission electron microscopy (cryo-TEM) micrograph of Empty Lip and LipRosi; scale bar = 100 nm.

The stability of LipRosi formulations (suspended in PBS) over time, stored at 4°C, was evaluated for 3 months and examined periodically for size, PDI, and zeta potential changes. Insignificant changes in liposome size, PDI, and zeta potential were detected, <10nm, 0.008, and 4 mV, respectively (Fig. 2a-c). It should be noted that no leakage of rosiglitazone was observed after 2–3 weeks of storage. Further studies evaluated the possible leakage of rosiglitazone in terms of the liposomal formulation's

physicochemical properties, such as insignificant changes in liposome size, PDI, and zeta potential.

Adsorption of serum proteins could change the biodistribution and stability of liposomes. The effect of serum proteins on LipRosi and Empty Lip was examined using size changes following incubation in serum for up to 48 hr. Both formulations showed no changes in size, PDI, and zeta potential values (Fig. 2d).

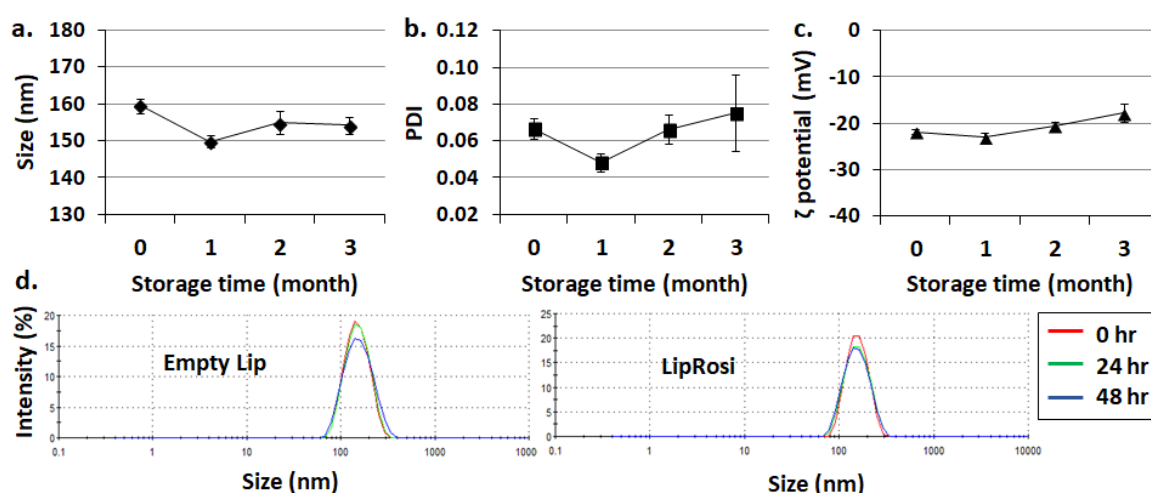


Figure 2. The stability of liposomal rosiglitazone (LipRosi) following incubation in PBS (a, b, c) and in fetal bovine serum (FBS) (d). The stability over time of LipRosi at 4°C was determined in terms of changes in size (a), PDI (b) and zeta potential (c). Data is presented as the mean±SD; n=3 at each time point. (d) Adsorption of proteins to LipRosi at 37°C (FBS incubation, diluted 1:100) was determined before incubation (red line), and after 24 and 48 hr incubation (green and blue line, respectively) in comparison to Empty Lip evaluated by measuring size distribution.

Bioactivity

The inhibitory effect of LipRosi on monocyte depletion in vitro was examined in RAW 264.7 cells culture (a monocytes/macrophages cell line). Free Rosi (0.1 mM) and Empty Lip (same

lipids concentration) treatments had no effect at both incubation times (24 and 48 hr; viability > 80%; Fig. 3). In contrast, LipRosi (0.1 mM) significantly inhibited RAW 264.7 cells proliferation, 39.5% and 79%, after 24 and 48 hr, respectively (Fig. 3).

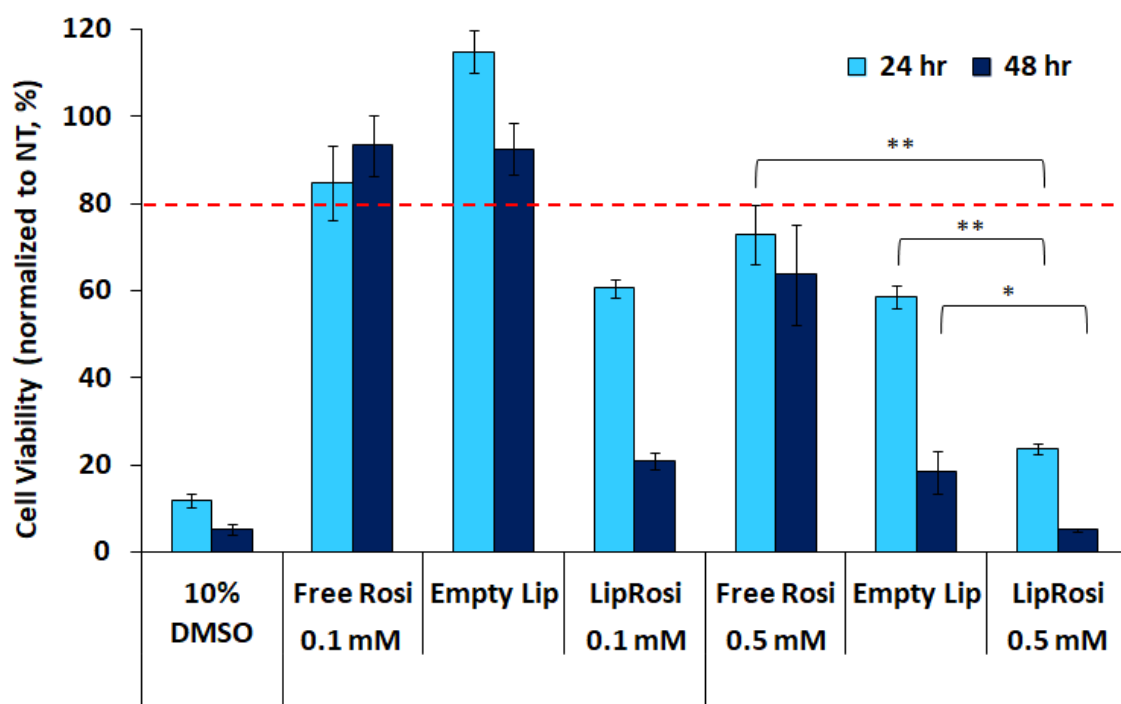


Figure 3. Time- and concentration-dependent inhibition of monocytes (RAW 264.7; monocyte/macrophage cell line) by liposomal rosiglitazone (LipRosi) in comparison to empty liposomes (Empty Lip) and rosiglitazone in solution (pH 4 solution; Free Rosi). Cells were treated with LipRosi (lipid concentration of 0.43 and 2.17 mg/ml; rosiglitazone concentration of 0.1 and 0.5 mM, respectively), Empty Lip (same lipids concentration) and Free Rosi (0.1 and 0.5 mM). Bioactivity was evaluated by the MTT assay and is expressed as % of untreated cells. Results are presented as mean±SD; The dotted line represents the upper level of cells viability; * $p < 0.05$, Empty Lip vs. LipRosi at 48 hr; ** $p < 0.01$, Free Rosi vs. LipRosi and Empty Lip vs. LipRosi at 24 hr

Upon increasing drug concentration treatment (0.5 mM), cells treated with Free Rosi solution exhibited a modest effect after 24 hr and 48 hr (27% and 36%, respectively). In contrast, LipRosi (0.5 mM) treatment significantly affected cell viability compared to all treatments. After 24 hr and 48 hr of incubation, treatment with LipRosi resulted in 76% and 95% reduction in cell proliferation, compared to treatment with Empty Lip (40% and 82%, respectively; Fig. 3).

Uptake by monocytes in culture

Cellular uptake of LipRosi by the monocytes/macrophages cell line, RAW 264.7, was examined by confocal microscopy of liposomes labeled with Cy5 and rhodamine, core, and membrane labeling, respectively. After 4 hr of incubation, the liposomes were detected within the cells (Fig. 4). Increased accumulation over time of LipRhod-Cy5 in cells was observed at both concentrations (Fig. 4 and Fig. S3), and liposomes were engulfed by the entire cell population after 24 hr at the highest examined concentration.

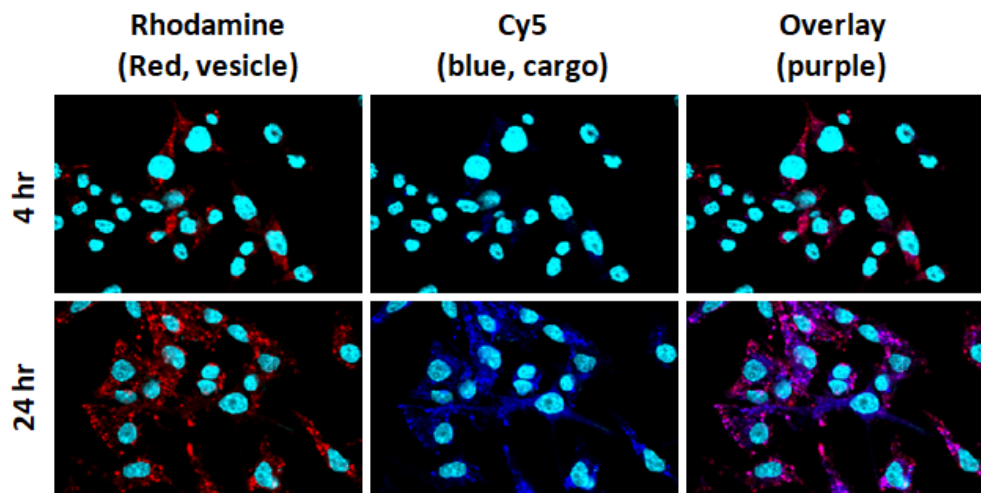


Figure 4. Qualitative assessment of fluorescently-labeled liposomes (rhodamine and Cy5, aqueous core and membrane, respectively; LipRhod-Cy5; 1.25 mg/ml lipids concentration) uptake by RAW264.7 cells. The nuclei are shown in turquoise (Hoechst), liposomes bilayer is shown in red (PE-Rhodamine), liposomes cargo is shown in blue (Cy5), and overlay of vesicle and cargo is shown in purple. The release of the aqueous core marker, Cy5, can be observed in the cytosol by the diffusive form of the dye, as opposed to the red spotted dye, which depicts the membrane marker. Images were obtained by means of confocal microscopy and analyzed with FV10-ASW 3.1 viewer software. The fluorescence intensity is normalized to non-treated cells; magnification x60 nm.

Cytotoxicity

Empty Lip was found to be non-toxic at all concentrations and time points examined (Fig. 5). In contrast, the cells' viability decreased gradually by increasing Free Rosi or LipRosi concentrations and incubation times. Free Rosi and LipRosi (0.1 mM) treatments exhibited a

cytotoxic effect (viability < 80%) 48 hr after treatment. In contrast, 0.5 mM of Free Rosi and LipRosi treatments showed a cytotoxic effect after 24 hr of incubation. LipRosi treatment was found to have a greater effect on cells' viability (93% reduction) in comparison to Empty Lip and Free Rosi treatments (13% and 56%, respectively; $p < 0.01$; Fig. 5).

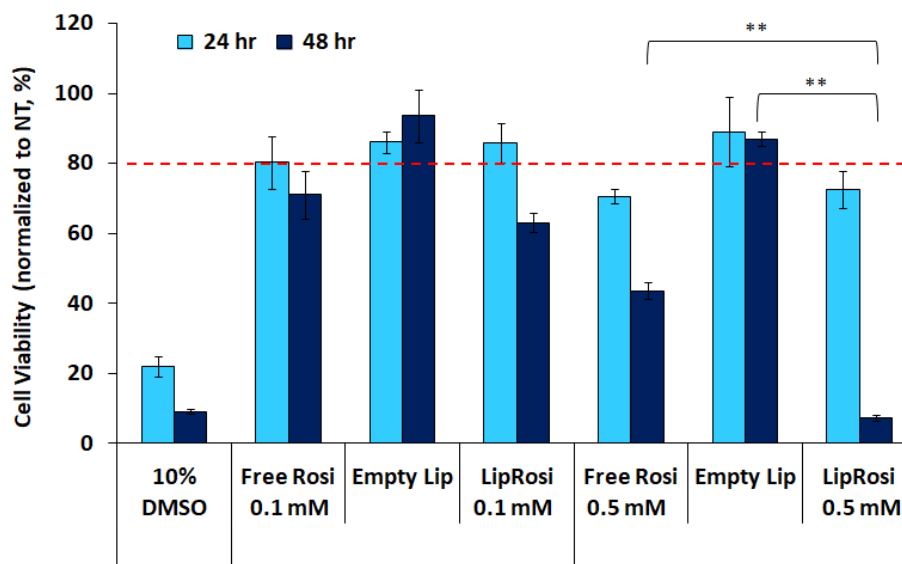


Figure 5. Time- and concentration-dependent cytotoxicity of liposomal rosiglitazone (LipRosi) in comparison to empty liposomes (Empty Lip) and rosiglitazone in solution (pH 4 solution; Free Rosi) on smooth muscle cells. Cells were treated with LipRosi (lipid concentration of 0.6 and 3 mg/ml; rosiglitazone concentration of 0.1 and 0.5 mM, respectively), Empty Lip (same lipid concentration) and Free Rosi (0.1 and 0.5 mM). Cytotoxicity was evaluated by the MTT assay and is expressed as % of untreated cells. Results are presented as mean \pm SD; The dotted line presents upper level of cells viability; $**p < 0.01$.

Biodistribution

The biodistribution of LipRosi in intact rats was evaluated following treatment with liposomes labeled with both rhodamine and Cy5

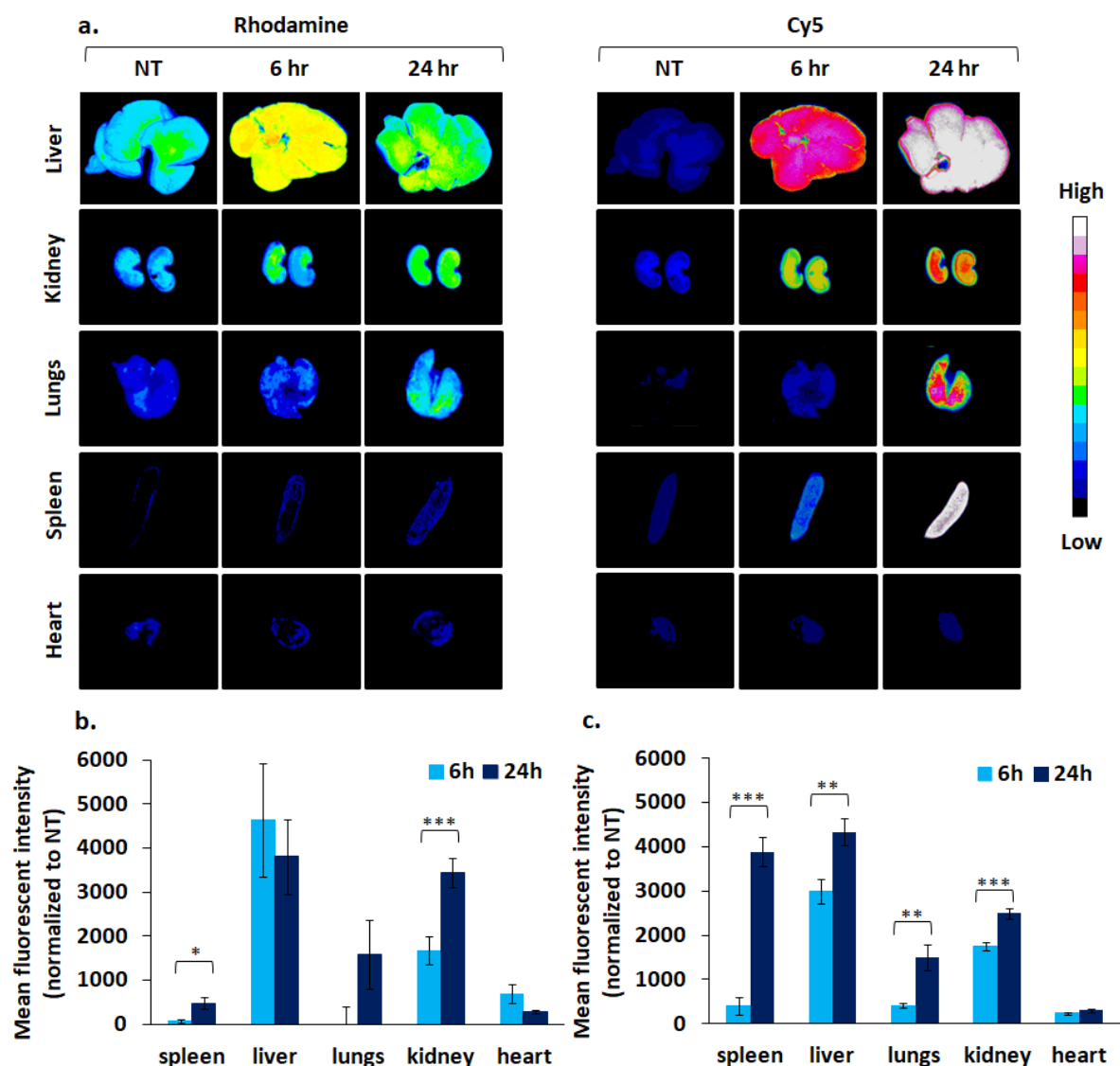


Figure 6. Qualitative (a) and quantitative (b and c) biodistribution of fluorescently-labeled empty liposomes (rhodamine and Cy5, aqueous core and membrane, respectively; LipRhod-Cy5) in rat organs, 6 and 24 hr after injection. Shown are pictures acquired by means of the Typhoon FLA followed by ImageJ analysis; $n=1$ for NT and $n=3$ for LipRhod-Cy5 at each time point. Data is presented as the mean \pm SEM; *** $p<0.001$, ** $p<0.01$, * $p<0.05$.

Only a negligible accumulation was detected in the heart, and accumulation in the spleen and lungs was minimal. After 24 hr, the biodistribution ranked, liver > kidney > lungs >> spleen and heart. Similarly, the rank was observed with Cy5 distribution at the same time, liver and spleen >> kidney > lungs > heart. In addition, the distribution of Cy5 24 hr post-injection was

(Fig. 6). Increased accumulation of rhodamine was observed in the liver in comparison to other organs after 6 hr ($p<0.01$; Fig. 6b).

found to be significantly higher than that after 6 hr in all organs (** $p<0.01$ and *** $p<0.001$), except for the heart (Fig. 6c).

Uptake of LipRosi by WBC in vivo

The uptake of LipRosi by circulating WBC was evaluated using FACS (Fig. 7).

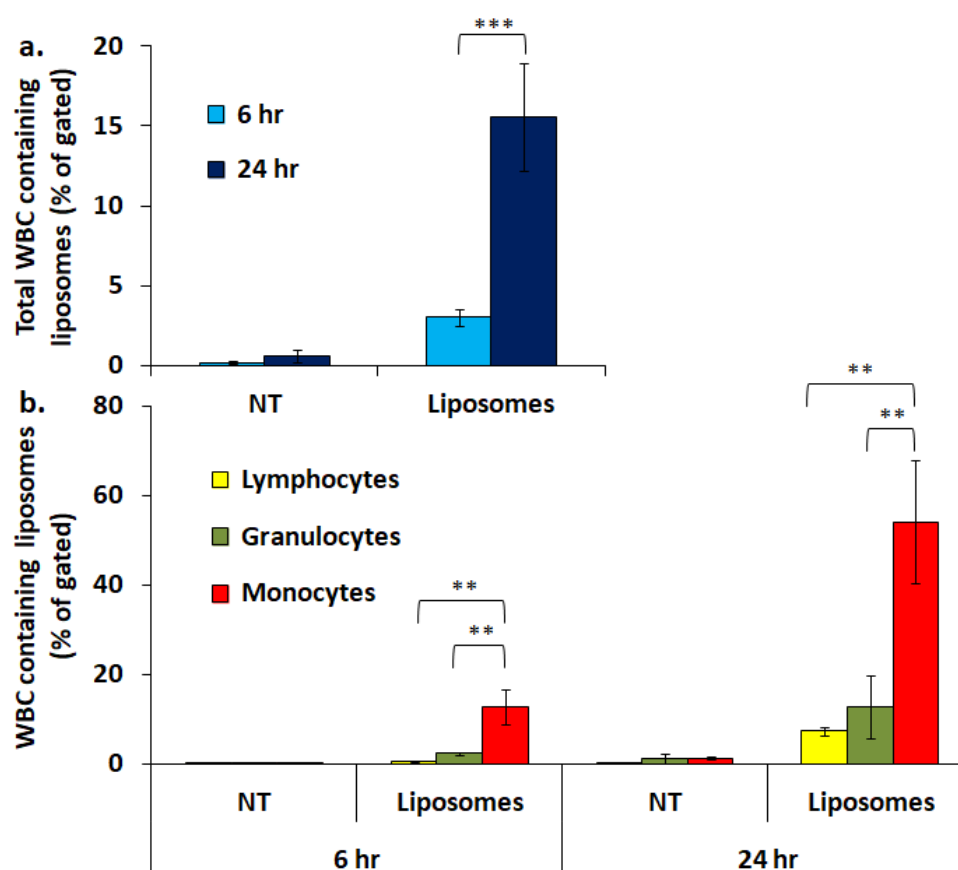


Figure 7. Time-dependent uptake of fluorescently-labeled empty liposomes (rhodamine and Cy5, aqueous core and membrane, respectively) by circulating white blood cells (WBC) in rats. (a) Total Cy5 labeled WBC. (b) Cy5 labeled lymphocytes, granulocytes and monocytes. Uptake was evaluated by means of flow cytometry. $n=1$ for NT and $n=3$ for LipRhod-Cy5 at each time point. Data is presented as the mean \pm SD; ** $p<0.01$, *** $p<0.001$.

Rhodamine labeled WBC could not be detected due to false-positive coloring, and only negligible background Cy5 fluorescence was detected in untreated rats. LipRosi uptake by WBC increased significantly 24 hr after treatment compared to the levels obtained after 6 hr ($3.03\pm0.55\%$ vs. $15.58\pm3.36\%$; *** $p<0.001$; Fig. 7a).

Liposomes uptake by monocytes was significantly higher than by lymphocytes and granulocytes gated cells at both time points (** $p<0.01$; Fig. 7b). After 6 hr, $12.83\pm4.01\%$ of gated monocytes contained liposomes while negligible uptake was detected in lymphocytes and granulocytes. After 24 hr, monocyte uptake increased significantly to $54.16\pm13.7\%$, whereas only $7.36\pm0.86\%$ and $12.9\pm6.96\%$ were internalized by lymphocytes and granulocytes, respectively.

Monocytes depletion in vivo

The effect of LipRosi on circulating monocytes was evaluated in rats following IV injection through flow cytometry. In two separate experiments, rats were treated with a dose of 10 mg/kg or 20 mg/kg on day 0, and monocyte levels were examined on three consecutive days post injection (Fig. S4a). No significant reduction of monocyte levels was observed following treatment with 10 mg/kg LipRosi; both saline and LipRosi treated groups tended to increase monocyte levels (Fig. S4b). Conversely, reduced monocyte levels were observed 24 and 48 hr following treatment with 20 mg/kg LipRosi (without reaching statistical significance) (Fig. S4c), returning to baseline levels after 72 hr.

Since no significant activity was detected following a single dose, rats were treated with 20 mg/kg LipRosi on two consecutive days (on day -1 and day 0; see scheme, Fig. 8a).

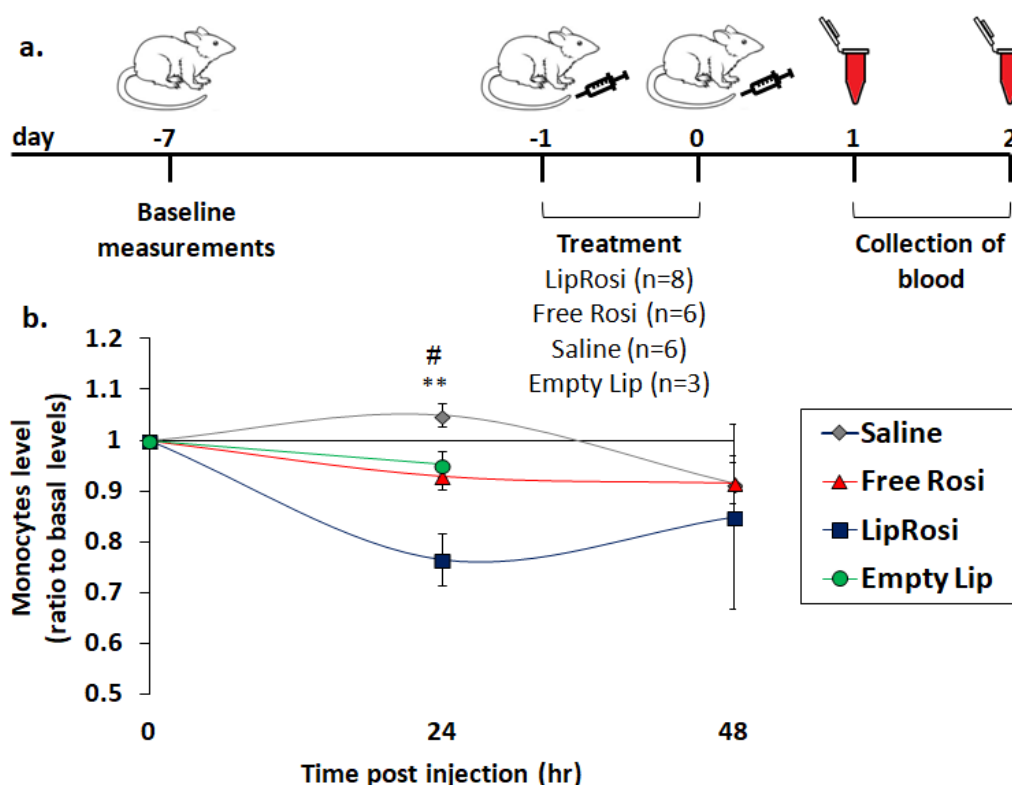


Figure 8. The inhibition of rat's circulating monocytes following IV injection of liposomal rosiglitazone (20 mg/kg) in two consecutive days. **(a)** Schematic presentation of animal experimental setup. **(b)** Monocytes levels measured in the blood a week before injection (baseline, 0 hr), 24 and 48 hr post two injections (IV) by means of flow cytometry. Monocytes were defined as ED1-positive (CD68) cells and are presented as the ratio normalized to the individual baseline level. Data is presented as the mean \pm SEM. $n=3-4$ animals in each group. ** $p<0.01$, LipRosi vs. saline; # $p<0.05$, LipRosi vs. Empty Lip.

Treatment with LipRosi by 2 injections exerted a significant depletion of monocytes in comparison to saline treatment (23% reduction vs. 5% increase from the basal level; $p<0.01$; Fig. 8b). In contrast, no significant depletion was detected following both Free Rosi and Empty Lip treatments (7% and 5%, respectively).

Discussion

Our work's premise is to utilize a drug's known polypharmacology properties to unlock novel therapeutic opportunities by redesigning its drug delivery system (28). Rosiglitazone is a proven, highly effective drug in treating type II diabetes mellitus. Nevertheless, the EMA suspended the drug, and the FDA restricted its clinical use due to cardiovascular-specific toxicity and increased mortality risk (15-17). Importantly, rosiglitazone has been shown to exert potent anti-inflammatory effects (20-23). Therefore, we thought to repurpose rosiglitazone

as an anti-inflammatory agent by re-routing its biodistribution away from the heart towards monocytes/macrophages. Besides their role as scavengers and in immune and non-immune defense mechanisms, monocytes/macrophages play a key role in the inflammatory cascade. Upon inflammatory stimuli, the number of circulating monocytes and their migration to the site of inflammation increase dramatically. It is well known that NPs are readily taken up by phagocytic cells of the MPS, monocytes/macrophages in particular, and to some extent by neutrophils. Therefore, NPs can enhance the intracellular delivery of an anti-inflammatory drug into phagocytic innate-immune cells for therapeutic means, as demonstrated in various inflammatory-associated disorders (1, 10-13, 26, 29, 30). In this study, we used the phagocytic nature of MPS cells to our advantage, developing a monocyte-targeted liposomal formulation containing rosiglitazone.

The governing physicochemical factors of MPS-targeted liposomes include surface charge

(positive or negative) and size (31-33). Negatively-charged particles in the range of 80–200 nm are preferable due to the suitable compromise between high phagocytic capability by the MPS and lower systemic toxicity, as well as the possibility for filter sterilization (26, 32, 34). In addition, the optimal formulation should possess a high drug loading capacity and a sufficient encapsulation yield.

In this study, multiple attempts were made to incorporate rosiglitazone in the aqueous core by the thin film hydration technique and by additional procedures, including the freeze and thaw method (25, 35, 36). Although attempts using the passive loading method resulted in formulations with optimal surface charge and size, the active loading method yielded a higher drug encapsulation level, two times higher than that obtained by the passive loading method (0.6 mg/ml vs. 1.15 mg/ml; compare Fig. S1 to Fig. S2a). Several parameters have been examined for obtaining an optimal formulation, including membrane rigidity (Fig. S2a), calcium acetate concentration in the hydrating solution (Fig. S2b), remote-loaded drug concentration (Fig. S2c), and time (Fig. S2d). The developed negatively-charged rosiglitazone formulation (LipRosi) possessed appropriate physicochemical properties, including a nano-size range with a low PDI (~170 nm; PDI, 0.075; Table 1) and both high drug loading (5.1 mg/ml) and encapsulation yield (~50%). In addition, the formulation manifested stable shelf life (over 3 months; Fig. 2a-c).

Morphologically, LipRosi appeared as a unique elongated ellipsoid vesicle (Fig. 1). A vesicle's shape is known to be influenced by osmotic gradients across the membrane, resulting in elongated and tubular structures (37, 38). Therefore, it is suggested that the complex of rosiglitazone with calcium in the vesicle's core precipitates due to its low solubility, altering the morphology of the liposome. In addition, the membrane's curvature is most likely affected to some extent by the association of the drug with the membrane lipids. Supporting this explanation is the drug's affinity to the lipid phase reflected by its logP of ~3 (39).

Serum protein absorption onto the liposome membrane could affect its phagocytosis, biological fate, biodistribution, and stability (40). Nevertheless, no difference in the mean size and PDI of LipRosi and Empty Lip was noted

following incubation in FBS (Fig. 2d). Thus, it is expected that the formulation will not be affected in vivo by the adsorption of serum proteins. Indeed, in comparison to lymphocytes and granulocytes, preferential uptake by monocytes was observed in vivo (Fig. 7b).

LipRosi was examined in vitro for its bioactivity, uptake, and cytotoxicity, using RAW264.7 (monocytes/macrophages line) and rat SMC cultures. At low drug concentrations (0.1 mM), only LipRosi treatment resulted in the inhibition of monocytes. However, at a higher drug concentration of 0.5 mM, all treatments showed a time-dependent bioactivity effect (Fig. 3), and LipRosi was the most potent treatment. The slight effect of Empty Lip in vitro corresponds with previous findings (26). The results confirm that the inhibitory effect of rosiglitazone on monocytes/macrophages, which is time- and concentration-dependent, is significantly improved by encapsulating it in liposomes.

Cellular uptake of the liposomal formulation was studied with liposomes double-labeled with rhodamine and Cy5 (membrane and inner aqueous core, respectively). A time- and dose-dependent uptake of LipRhod-Cy5 was found (Fig. 4 and Fig.S3). As expected, the entire cell population was eventually internalized since monocytes are phagocytic cells. After 24 hr, a diffusive form of Cy5 in the cytoplasm was observed, indicating its release from the liposomal aqueous core and subsequently from the lysosome. In the increased concentration examined, more vesicles were available for phagocytosis (Fig. 4 vs. Fig.S3), most probably dependent on the number of vesicles, as we have previously demonstrated (41).

LipRosi and Free Rosi were found to have a dose- and time-dependent cytotoxic effect when examined on rat SMC (Fig. 5). The cytotoxic effect of free rosiglitazone on SMC is in accord with its anti-proliferative properties (42, 43). The apparent cytotoxic effects of LipRosi observed in the SMC culture studies occurred at the highest concentration and after an extended incubation period, allowing rosiglitazone to internalize and exert its bioactivity. Nevertheless, no clinical signs of toxicity were observed in animal studies (see below).

The fate and biodistribution of the fluorescently double-labeled formulation were examined following LipRhod-Cy5 administration via the tail vein in male sabra rats. An increased accumulation over time of LipRhod-Cy5 in all harvested organs was found, with the liver, a macrophage-rich organ, showing the highest accumulation (Fig. 6). This confirms our working hypothesis that the formulated liposomes are mainly internalized by monocytes/macrophages, and consequently accumulate in the liver. Notably, only limited accumulation was noted in the heart. In addition, a significant time-dependent accumulation in the Cy5 channel could be seen in all harvested organs except the heart (Fig. 6c). This underscores the significant advantage of the proposed delivery system in minimizing or potentially altogether avoiding the side effects that have led to the market withdrawal of rosiglitazone or its label warning. The significant increase in the mean fluorescent intensity of Cy5 over time is attributed to the release of the fluorescent dye from the aqueous core, as was observed *in vitro* (Fig. 4).

The bioactivity effect on monocytes/macrophages *in vitro* suggested that monocyte depletion *in vivo* could be achieved. Several dose-response experiments have been carried out to exceed the threshold effect (Fig. S4). Finally, administration of 20 mg/kg LipRosi, injected on two consecutive days, resulted in significant inhibition of circulating monocytes after 24 hr (Fig. 8). In contrast, Empty Lip had no influence on monocytes depletion, indicating that the effect is attributed to the drug in its encapsulated form. Furthermore, depletion of monocytes by LipRosi *in vivo* was more effective than the free drug (borderline significance), showing the same pattern as the *in vitro* results (Fig. 3). This is in accord with the known effective uptake of particulate dosage forms by monocytes (33), and was further demonstrated by the *in vivo* internalization study where a significantly higher uptake was observed compared to both lymphocytes and granulocytes (Fig. 7b).

Perspectives and limitations

Previous studies by our group demonstrated that partial and transient depletion of circulating monocytes by systemic administration of liposomes containing various bisphosphonates, which are in clinical use for the treatment of bone-related disorders, is effective in the treatment of endometriosis in animal models (14, 29), and of arterial restenosis both in animals (11, 12, 14, 25, 26, 44, 45) and humans (46), with no side-effects. Similarly to liposomal bisphosphonates, LipRosi partially reduces circulating monocyte levels for two days (Fig. 8b), which could potentially impede the massive accumulation of monocytes into inflamed tissue. This treatment approach is particularly suitable when the intervention is at the early stages of monocyte/macrophage recruitment (47). Reduction of restenosis in animal models (rats and rabbits) is typically achieved with a single dose of 15 mg/kg or 3 mg/kg, respectively, of liposomal alendronate (a bisphosphonate) (12, 25, 26, 44). For attenuating endometriosis in rats, multiple 4 once weekly injections of 10 mg/kg are required (29). Although liposomal alendronate seems more efficacious than LipRosi (1 injection of 15 mg/kg vs. 2 injections of 20 mg/kg), a side-by-side comparison in animal pathological models is required for proper comparison. As expected, the side effects observed with LipRosi application in the *in vitro* cell culture studies, at high concentration and extended incubation time, were not detected *in vivo*. In addition, a markedly lower single dose of 0.01 mg in patients with elevated basal blood levels of monocyte count yielded a significant reduction in late lumen loss with no side effects (46). Moreover, since various dosages of liposomal bisphosphonate treatment are associated with neither side effects (11, 12, 14, 25, 44) nor with complement activation (26), a similar profile of safety is expected with LipRosi, which was formulated with the same lipids and acts by the same mechanism of monocyte-targeting.

Conclusions

We endeavored to repurpose the effective but discouraged drug, rosiglitazone, for anti-inflammation therapy. A monocyte-targeted liposomal delivery system encapsulating rosiglitazone has been successfully formulated, characterized by desirable physicochemical properties for specific MPS disposition in terms of nano-size, narrow size distribution, negatively-charged membrane, high drug loading, and shelf-life stability. In vitro and in vivo studies showed that monocyte depletion by LipRosi was more potent than the free drug. The limited disposition of the liposomes detected in the heart suggests a safe drug delivery option for LipRosi. More studies should be conducted to further examine the impact of LipRosi in inflammation models and its possible systemic off-target effects.

Supporting Information

Supporting information can be downloaded from <https://precisionnanomedicine.com/article/38312>.

Conflict of interest

The authors have no relevant financial or non-financial interests to disclose. For signed statements contact the journal office edidor@precisionnanomedicine.com.

Acknowledgment

The Cryo-TEM work was assisted by Dr. Yael Levi-Kalishman at the Hebrew University Center for Nanoscience and Nanotechnology. This study is part of OS' MSc thesis. The authors declare no conflict of interest associated with this publication.

Refer to this article as Shvindelman O, Nordling-David MM, Grad E, and Golomb G, Harnessing Monocytes for a Liposomal Rosiglitazone-Mediated Anti-Inflammatory Effect, *Precis. Nanomed.* 2022 5(4):930-945, <https://doi.org/10.33218/001c.38312>

References

1. Gutman D, Golomb G. Liposomal alendronate for the treatment of restenosis. *J Control Release.* 2012;161(2):619-627.
2. Silva MT, Correia-Neves M. Neutrophils and macrophages: the main partners of phagocyte cell systems. *Front Immunol.* 2012;3:174.
3. van Furth R, Cohn ZA, Hirsch JG, Humphrey JH, Spector WG, Langevoort HL. The mononuclear phagocyte system: a new classification of macrophages, monocytes, and their precursor cells. *Bull World Health Organ.* 1972;46(6):845-852.
4. Aizik G, Grad E, Golomb G. Monocyte-mediated drug delivery systems for the treatment of cardiovascular diseases. *Drug Deliv Transl Res.* 2018;8(4):868-882.
5. Gordon S, Taylor PR. Monocyte and macrophage heterogeneity. *Nat Rev Immunol.* 2005;5(12):953-964.
6. Ponzoni M, Pastorino F, Di Paolo D, Perri P, Brignole C. Targeting macrophages as a potential therapeutic intervention: impact on inflammatory diseases and cancer. *Int J Mol Sci.* 2018;19(7).
7. Ashley NT, Weil ZM, Nelson RJ. Inflammation: mechanisms, costs, and natural variation. *Annu Rev Ecol Evol S.* 2012;43:385-406.
8. Hotamisligil GS. Inflammation and metabolic disorders. *Nature.* 2006;444(7121):860-867.
9. Kinne RW, Brauer R, Stuhlmuller B, Palombo-Kinne E, Burmester GR. Macrophages in rheumatoid arthritis. *Arthritis Res.* 2000;2(3):189-202.
10. Cohen-Sela E, Rosenzweig O, Gao J, Epstein H, Gati I, Reich R, Danenberg HD, Golomb G. Alendronate-loaded nanoparticles deplete monocytes and attenuate restenosis. *J Control Release.* 2006;113(1):23-30.
11. Danenberg HD, Fishbein I, Gao J, Monkkonen J, Reich R, Gati I, Moerman E, Golomb G. Macrophage depletion by clodronate-containing liposomes reduces neointimal formation after balloon injury in rats and rabbits. *Circulation.* 2002;106(5):599-605.

12. Danenberg HD, Golomb G, Groothuis A, Gao J, Epstein H, Swaminathan RV, Seifert P, Edelman ER. Liposomal alendronate inhibits systemic innate immunity and reduces in-stent neointimal hyperplasia in rabbits. *Circulation*. 2003;108(22):2798-2804.
13. Barrera P, Blom A, van Lent PL, van Bloois L, Beijnen JH, van Rooijen N, de Waal Malefijt MC, van de Putte LB, Storm G, van den Berg WB. Synovial macrophage depletion with clodronate-containing liposomes in rheumatoid arthritis. *Arthritis Rheum*. 2000;43(9):1951-1959.
14. Haber E, Afergan E, Epstein H, Gutman D, Koroukhov N, Ben-David M, Schachter M, Golomb G. Route of administration-dependent antiinflammatory effect of liposomal alendronate. *J Control Release*. 2010;148(2):226-233.
15. EMA. European Medicines Agency recommends suspension of Avandia, Avandamet and Avaglim. Available from: https://www.ema.europa.eu/en/documents/press-release/european-medicines-agency-recommends-suspension-avandia-avandamet-avaglim_en.pdf.
16. Nissen SE. The rise and fall of rosiglitazone. *Eur Heart J*. 2010;31(7):773-776.
17. Wallach JD, Wang K, Zhang AD, Cheng DN, Nardini HK, Lin HQ, Bracken MB, Desai M, Krumholz HM, Ross JS. Updating insights into rosiglitazone and cardiovascular risk through shared data: individual patient and summary level meta-analyses. *Bmj-Brit Med J*. 2020;368.
18. Silvio E Inzucchi M, Beatrice Lupsa, MD. Thiazolidinediones in the treatment of type 2 diabetes mellitus. UptoDate. Available from: <https://www.uptodate.com/contents/thiazolidinediones-in-the-treatment-of-type-2-diabetes-mellitus>.
19. Heming M, Gran S, Jauch SL, Fischer-Riepe L, Russo A, Klotz L, Hermann S, Schafers M, Roth J, Barczyk-Kahlert K. Peroxisome proliferator-activated receptor-gamma modulates the response of macrophages to lipopolysaccharide and glucocorticoids. *Front Immunol*. 2018;9:893.
20. Jiang C, Ting AT, Seed B. PPAR-gamma agonists inhibit production of monocyte inflammatory cytokines. *Nature*. 1998;391(6662):82-86.
21. Reddy RC. Immunomodulatory role of PPAR-gamma in alveolar macrophages. *J Investig Med*. 2008;56(2):522-527.
22. Ricote M, Li AC, Willson TM, Kelly CJ, Glass CK. The peroxisome proliferator-activated receptor-gamma is a negative regulator of macrophage activation. *Nature*. 1998;391(6662):79-82.
23. Mohanty P, Aljada A, Ghanim H, Hofmeyer D, Tripathy D, Syed T, Al-Haddad W, Dhindsa S, Dandona P. Evidence for a potent anti-inflammatory effect of rosiglitazone. *J Clin Endocrinol Metab*. 2004;89(6):2728-2735.
24. Hironaka K, Inokuchi Y, Fujisawa T, Shimazaki H, Akane M, Tozuka Y, Tsuruma K, Shimazawa M, Hara H, Takeuchi H. Edaravone-loaded liposomes for retinal protection against oxidative stress-induced retinal damage. *Eur J Pharm Biopharm*. 2011;79(1):119-125.
25. Epstein H, Gutman D, Cohen-Sela E, Haber E, Elmalak O, Koroukhov N, Danenberg HD, Golomb G. Preparation of alendronate liposomes for enhanced stability and bioactivity: in vitro and in vivo characterization. *AAPS J*. 2008;10(4):505-515.
26. Epstein-Barash H, Gutman D, Markovsky E, Mishan-Eisenberg G, Koroukhov N, Szebeni J, Golomb G. Physicochemical parameters affecting liposomal bisphosphonates bioactivity for restenosis therapy: internalization, cell inhibition, activation of cytokines and complement, and mechanism of cell death. *J Control Release*. 2010;146(2):182-195.
27. Xu S, Fu J, Chen J, Xiao P, Lan T, Le K, Cheng F, He L, Shen X, Huang H, Liu P. Development of an optimized protocol for primary culture of smooth muscle cells from rat thoracic aortas. *Cytotechnology*. 2009;61(1-2):65-72.
28. Krishnamurthy N, Grimshaw AA, Axson SA, Choe SH, Miller JE. Drug repurposing: a systematic review on root causes, barriers and facilitators. *BMC Health Serv Res*. 2022;22(1):970.
29. Haber E, Danenberg HD, Koroukhov N, Ron-El R, Golomb G, Schachter M. Peritoneal macrophage depletion by liposomal bisphosphonate attenuates endometriosis in the rat model. *Hum Reprod*. 2009;24(2):398-407.
30. Gutman D, Epstein H, Koroukhov N, Golomb G. Liposomal delivery system of adenosine for modulating inflammation. *J Drug Deliv Sci Tec*. 2009;19(4):257-262.

31. Doshi N, Mitragotri S. Macrophages recognize size and shape of their targets. *Plos One*. 2010;5(3).
32. Li SD, Huang L. Pharmacokinetics and biodistribution of nanoparticles. *Mol Pharm*. 2008;5(4):496-504.
33. Kelly C, Jefferies C, Cryan SA. Targeted liposomal drug delivery to monocytes and macrophages. *J Drug Deliv*. 2011;2011:727241.
34. Afergan E, Ben David M, Epstein H, Koroukhov N, Gilhar D, Rohekar K, Danenberg HD, Golomb G. Liposomal simvastatin attenuates neointimal hyperplasia in rats. *AAPS J*. 2010;12(2):181-187.
35. Costa AP, Xu X, Burgess DJ. Freeze-anneal-thaw cycling of unilamellar liposomes: effect on encapsulation efficiency. *Pharm Res*. 2014;31(1):97-103.
36. Gubernator J. Active methods of drug loading into liposomes: recent strategies for stable drug entrapment and increased in vivo activity. *Expert Opin Drug Deliv*. 2011;8(5):565-580.
37. Abraham SA, Edwards K, Karlsson G, MacIntosh S, Mayer LD, McKenzie C, Bally MB. Formation of transition metal-doxorubicin complexes inside liposomes. *Biochim Biophys Acta*. 2002;1565(1):41-54.
38. Ron-Doitch S, Sawodny B, Kuhbacher A, David MMN, Samanta A, Phopase J, Burger-Kentischer A, Griffith M, Golomb G, Rupp S. Reduced cytotoxicity and enhanced bioactivity of cationic antimicrobial peptides liposomes in cell cultures and 3D epidermis model against HSV. *J Control Release*. 2016;229:163-171.
39. IARC working group on the evaluation of carcinogenic risk to humans. Some drugs and herbal products; 2016.
40. Bonte F, Juliano RL. Interactions of liposomes with serum proteins. *Chem Phys Lipids*. 1986;40(2-4):359-372.
41. Aizik G, Waiskopf N, Agbaria M, Levi-Kalisman Y, Banin U, Golomb G. Delivery of liposomal quantum dots via monocytes for imaging of inflamed tissue. *ACS Nano*. 2017;11(3):3038-3051.
42. Wang K, Zhou Z, Zhang M, Fan L, Forudi F, Zhou X, Qu W, Lincoff AM, Schmidt AM, Topol EJ, Penn MS. Peroxisome proliferator-activated receptor gamma down-regulates receptor for advanced glycation end products and inhibits smooth muscle cell proliferation in a diabetic and nondiabetic rat carotid artery injury model. *J Pharmacol Exp Ther*. 2006;317(1):37-43.
43. Little PJ, Osman N, de Dios ST, Cemerlang N, Ballinger M, Nigro J. Anti-proliferative activity of oral anti-hyperglycemic agents on human vascular smooth muscle cells: thiazolidinediones (glitazones) have enhanced activity under high glucose conditions. *Cardiovasc Diabetol*. 2007;6:33.
44. Danenberg HD, Fishbein I, Epstein H, Waltenberger J, Moerman E, Monkkonen J, Gao J, Gathi I, Reichi R, Golomb G. Systemic depletion of macrophages by liposomal bisphosphonates reduces neointimal formation following balloon-injury in the rat carotid artery. *J Cardiovasc Pharmacol*. 2003;42(5):671-679.
45. Grad E, Zolotarevsky K, Danenberg HD, Nordling-David MM, Gutman D, Golomb G. The role of monocyte subpopulations in vascular injury following partial and transient depletion. *Drug Deliv Transl Res*. 2018;8(4):945-953.
46. Banai S, Finkelstein A, Almagor Y, Assali A, Hasin Y, Rosenschein U, Apruzzese P, Lansky AJ, Kume T, Edelman ER. Targeted anti-inflammatory systemic therapy for restenosis: the bioresorbable liposomal alendronate with stenting sTudy (BLAST)-a double blind, randomized clinical trial. *Am Heart J*. 2013;165(2):234-240 e231.
47. Welt FG, Rogers C. Inflammation and restenosis in the stent era. *Arterioscler Thromb Vasc Biol*. 2002;22(11):1769-1776.